International Journal of Innovative Research and Scientific Studies, 8(3) 2025, pages: 2817-2833

IJIRSS
International Journal of Innovative Research & Scientific Studies

ISSN: 2617-6548

URL: www.ijirss.com

DeepSystem: The Effect of the Optimized Deep Learning and Blurring Filters on the Automated Detection of Pneumonia Using X-ray Images

Suleyman A. AlShowarah[1*], Aymen I. Zreikat[2], Hisham Al Assam[3]

[1]*Department of Software Engineering, Faculty of Information Technology, Mutah University, Al-Karak, Jordan.*
[2]*College of Engineering and Technology, American University of the Middle East Kuwait.*
[3]*School of Computing, The University of Buckingham, UK.*

Corresponding author: Suleyman A. AlShowarah (*Email: showarah@mutah.edu.jo*)

Abstract

Pneumonia is a potentially fatal respiratory infection affecting a significant portion of the population, particularly in areas with high pollution, overcrowding, poor sanitary conditions, and limited healthcare infrastructure. Pneumonia typically leads to pericardial effusion, a condition in which fluid fills the chest and causes breathing problems. Timely and accurate diagnosis of pneumonia is vital for effective treatment that improves the probabilities of survival. Specialists can detect pneumonia manually, but the process is time-consuming and prone to human error, making it inefficient for processing huge volumes of images. Automated detection systems for pneumonia can significantly streamline this process. This study investigates the power of deep learning to develop predictive models for accurate pneumonia detection using chest X-rays. It examines the impact of several factors on classification accuracy using ResNet-50 and Inception V3 as deep feature extraction models. These factors include the effect of applying four common image filters on classification accuracy, the influence of using a dropout layer, and the impact of employing different classifiers, i.e., Support Vector Machine (SVM), Random Forest (RF), and Naïve Bayes (NB). The findings reveal that, although the results across all models and filters were comparable, ResNet-50 combined with SVM scored the highest accuracy of 98% when using the Gaussian filter. Similarly, Inception V3 with SVM provided high classification accuracy, achieving 98% with both the Gaussian filter and the original data. However, the performance of the Median filter (using Skimage) showed improvement with Inception V3 compared to ResNet-50. These findings underscore the importance of selecting suitable image filters and deep learning models to optimize classification performance. Moreover, SVM consistently outperformed both RF and NB across all datasets, confirming its effectiveness as the most reliable classifier in this context.

Keywords: Pneumonia detection, Image filters, Data augmentation, Deep learning algorithms, Dropout layer.

DOI: 10.53894/ijirss.v8i3.7087
Funding: This study received no specific financial support.
History: Received: 27 March 2025 / **Revised:** 1 May 2025 / **Accepted:** 6 May 2025 / **Published:** 16 May 2025

Competing Interests: The authors declare that they have no competing interests.
Authors' Contributions: All authors contributed equally to the conception and design of the study. All authors have read and agreed to the published version of the manuscript.

Transparency: The authors confirm that the manuscript is an honest, accurate, and transparent account of the study; that no vital features of the study have been omitted; and that any discrepancies from the study as planned have been explained. This study followed all ethical practices during writing.
Publisher: Innovative Research Publishing

1. Introduction

Pneumonia is a major global health concern, responsible for high mortality rates worldwide. It is one of the most common types of viral infections [1] caused by viruses or bacteria that compromise lung function [2, 3]. It is a leading cause of death among children; 99% of deaths in children who are under 5 years of age [4] as well as among the elderly (over 65 years) in developed countries [5-7]. According to the statistical data and key facts about the pneumonia that was issued on October 3, 2023, it says that there are around one billion cases of seasonal pneumonia annually, including 3 to 5 million cases classified as severe illness [4]. Moreover, it is estimated to cause between 290.000 to 650.000 respiratory deaths annually [4]. Approximately 7% of the world population is infected by pneumonia each year and an estimated 4 million deaths [8].

Recently, the outbreak of the new SARS-CoV-2 virus has caused a great deal of chaos around the world. Today, there are more than 702 million confirmed cases of the virus worldwide, resulting deaths of people about 6.9 million [9]. In most cases, SARS-CoV-2 causes pneumonia [10]. At times, medical systems in most countries become overwhelmed by the large numbers of infected patients [11]. In light of these challenges, rapid and reliable pneumonia diagnosis is essential for timely treatment and better outcomes.

Standard diagnostic tools for diagnosing pneumonia include chest X-rays (CXRs), CT, MRI, chest ultrasound, etc. [12]. Although chest X-ray is less sensitive in detecting pneumonia compared to other diagnostic tools i.e., chest CT and chest ultrasound [13, 14] but it is still considered a good tool for the diagnosis of pneumonia based on the guidelines of most clinical worldwide [15]. Furthermore, using chest X-ray machines are not expensive [13], faster to scan, available in most clinical, and compared to CT scans, chest X-ray machines have low radiation doses [15-17].

For highly effective treatment, accurate and early detection of pneumonia is critical. However, developing an accurate and timely detection system for pneumonia requires large volumes of labeled data, which cannot be easily available. Despite the availability of the current technology using radiological criteria and data, it requires specialists/ physicians to distinguish abnormalities, which is a challenging task. Therefore, it consumes physicians' time and efforts, and is prone to human error [18]. The data need to be labeled as well, whereas the available labeled images are limited [2].

In recent years, automated classification of medical images has witnessed tremendous growth in the healthcare field [19]. The automated process aims to detect pneumonia from medical images. Deep learning techniques, particularly convolutional neural networks (CNNs), have shown great promise in automating medical image classification [19]. These methods outperform traditional approaches by leveraging large datasets and advanced feature extraction capabilities [20-22].

Medical classification tasks are conducted using CNNs and ML algorithms [23]. CNNs excel in extracting features from diverse and complex images. The results achieved using CNNs for medical images benefit from advances in GPU hardware and transfer learning techniques in addition to the availability of labeled data. CNNs can be designed to extract features from chest X-rays to detect pneumonia and then used in classification accuracy [24]. The CNN model is able to accurately and timely classify pneumonia [25]. Hence, pneumonia can be treated at an early stage. Furthermore, DL will help to diagnose pneumonia in less time and minimize errors that may occur when diagnosed manually by experts. However, DL can work on large sizes of datasets [24, 25].

This research proposes a method to improve pneumonia diagnosis by implementing Deep Learning (DL) architectures enhanced with the Dropout regularization technique and four commonly used image filters: Gaussian, Bilateral, Median (Skimage), and Median using OpenCV filters. These filters are applied to reduce image noise and enhance feature visibility for more accurate classification [26, 27].

While most existing studies focus on CNN architectures and training strategies, few have examined the impact of image filters on CNN performance in medical image classification tasks [28]. In this study, we investigate the effect of preprocessing images using these filters before feeding them into a CNN for classification. The operator of Gaussian filter suppresses noise, therefore the edges of the image are smoothed, which affects edge detection accuracy [26]. While bilateral filter smooths images while preserving edges [27]. The following filters: Gaussian, Bilateral, Median using Skimage, and Median using Opencv are applied on the original images that results four new datasets to be classified.

In this research, features will be extracted from X-ray images using two well-known DL models, i.e., ResNet50 and Inception V3. In addition, four filters are applied to the original X-ray images; this is to investigate their influence on classification accuracy. Features are extracted from both the original chest X-ray images and the four additional datasets generated through the four image filters. The features are then classified using three Machine Learning (ML) algorithms: Support Vector Machine (SVM), Random Forest (RF), and Naïve Bayes (NB).

The proposed model is trained on augmented data to enhance generalizability, and a pooling layer is integrated into the proposed model architecture to reduce dimensionality. Then, a dropout layer (a regularization technique) is applied during model creation in some experiments of this study to prevent overfitting and improve the generalization ability of the model. Dropout is also excluded in some other experiments to measure its influence on classification accuracy as well.

At the final stage of the model, a single dense layer is employed to perform binary classification. This layer facilitates the generation of more compact and discriminative feature representations, helps mitigate overfitting, and improves classification accuracy. The use of a single dense layer also ensures consistency in the output dimensions across different CNN models (ResNet-50 and Inception V3) and filter configurations used in the study.

The key motivation for conducting this study is the urgent need to enhance pneumonia detection, a fundamental challenge in modern medicine that needs a very accurate and quick diagnosis. Traditional methods for diagnosing pneumonia usually rely heavily on expert knowledge for manual image interpretation, which is labor-intensive, time-consuming, and prone to human error, especially when dealing with large sizes of imaging data. Also Furthermore, according to publicly available statistical reports, pneumonia is increasing significantly since last five years [11]. limited number of studies investigating the role of image filters in pneumonia detection using chest X-rays provides additional motivation for this work, as it offers new insights to the existing body of literature. This research attempts to automate the pneumonia detection using DL techniques, particularly using Resnet50, and Inception V3. If it was successful, this approach could lead to earlier interventions, improved diagnostic accuracy, and reduced dependency on manual analysis. Ultimately, patients with pneumonia will benefit from this research, and the medical imaging analysis field will improve as a result. The potential impact of this research is important, as it has the potential to contribute to the establishment of effective and reliable tools for the healthcare providers [29]. The public availability of chest X-ray datasets further enables the development and validation of classification models, reinforcing the motivation behind this study to deliver a practical, accurate solution for pneumonia diagnosis [24].

The following contributions have been achieved through the development of the proposed model:

- A comprehensive framework integrating multiple processes for feature extraction, leveraging four image filters and data augmentation techniques, has been proposed to enhance classification results.
- A refined model architecture incorporating dense and Dropout layers to improve generalization and reduce overfitting.
- An extensive comparative analysis of the proposed model against various state-of-the-art methods using real-world datasets.
- Systematic evaluation of the data augmentation effect on classification accuracy.
- Assessing the impact of four distinct image filters on the accuracy of pneumonia classification.

The aim of the research can be accomplished by considering a number of objectives, as follows. 1) To develop a model that detects pneumonia based on X-ray images. 2) To investigate the performance of deep features and the efficacy of the machine learning classifiers on the reliably extracted features. 3) To evaluate the effect of the dropout layers on classification accuracy. 4) To verify whether improved accuracy results can be achieved by augmenting the sizes of the training datasets, and to examine the effect of four filters used on the X-ray images on classification accuracy.

The limitations of the study can be presented as follows. 1) The available studies on pneumonia detection. 2) It is challenging to find studies that investigate the effect of image filters on the results for pneumonia detection. 3) Limited studies have considered the efficiency performance of CNNs on filters like Median using OpenCV or Median using Skimage. 4) A detailed comparison of available studies shows that most of the applied datasets are unbalanced and very limited, providing unreliable results and presentation methods that are not suitable for widespread use.

The rest of the paper is organized as follows: In Section II, the most related works are reviewed. Section III presents the methodology. Experimental results are discussed in Section IV. Lastly, Section V provides the conclusion of the research.

2. Related Works

Over the past years, a number of studies have been conducted using different technologies to classify health images. Some of these studies were designed based on deep learning strategies, proposing methods to diagnose pneumonia utilizing chest X-ray images. For example, the researchers in Rajpurkar et al. [30] designed an approach named CheXNet. Their approach was trained on a dataset containing 14 different diseases; they applied their approach to 420 chest X-ray images. Their results in detecting pneumonia showed that deep learning achieved high average performance when compared to the performance of a radiologist. Researchers in Wu et al. [31] conducted a study to detect pneumonia using adaptive median filtering of CNN based on the Dropout layer, which was used to extract deep activation features from each chest X-ray image. They then employed a random forest. Adaptive filtering was applied to eliminate noise from the image, which would improve accuracy and facilitate the detection process. The Dropout layer was used for the CNN model with two layers. In order to improve the classification accuracy of convolutional neural networks, the researchers found that more preprocessing using adaptive filtering is needed. Additionally, a large dataset with labels is required for training data to improve accuracy. As a result, they found that transfer learning (TL) is proposed to solve the problem of the learning cost required for CNN architecture. Therefore, the use of transfer learning has become a very popular method, as it allows the CNN model to achieve high performance, minimize costs, and require less input [32]. The researchers in Ayan and Ünver [33] conducted a study using Xception and VGG-16 to fine-tune transfer learning. As the Xception design was changed by having two new fully connected layers and multiple output levels with the SoftMax activation. In theory, the base layer of the channel contains important information and potentially significant information. The first part of the eight-layer VGG-16 architecture was discontinued, and the fully connected layers were changed. This showed that the test time for the VGG-16 became 16ms and 20ms for the Xception per image.

The researchers in Chouhan et al. [34] conducted a study using InceptionV3, ResNet18, and GoogLeNet. The diagnosis for the images was designed as follows: classifiers were merged, then they used votes for the high proportion of the outcomes. This enhanced the test period, which required 161 milliseconds per image. So, the accuracy was enhanced in detecting the pneumonia. Transfer learning techniques are also used in Rahman et al. [35] on ImageNet to classify images based on pneumonia using four pre-trained CNN architectures. They conducted their study to classify chest radiography images using three classification strategies.

Few studies have investigated the influence of image' filters on CNN performance for medical image classification tasks, therefore, most of studies are focusing on CNN architectures and training methodologies when conducting their studies. The researchers in Das et al. [36] used preprocessing steps before feeding the images into a CNN for the classification task. These

filters included median and Gaussian filters. Their findings demonstrated that using the right filters may greatly increase classification accuracy. While the researchers in Monani et al. [28] investigated the effect of filters on the CNN performance using different filters like the Median filter, the Gaussian filter, the Adaptive median filter and the Wiener filter for medical image classification. They conducted the model on the publicly available datasets: Malaria, pneumonia and blood cell datasets. They found that the Wiener filter showed best performance for the malaria and pneumonia classification task with an accuracy of 96.57% and 96.93%, respectively. Whereas the Gaussian filter scored a high accuracy of 97.79% for Blood cell classification.

Various studies focused only on classification accuracy without considering preprocessing, dense layers, dropout layers, or the influence of using filters in their investigations. For example, the study in Ahuja et al. [37] conducted on ResNet18 based on dataset size contains 349 chest X-ray images. Their aim was to classify X-ray images as either pneumonia or non-pneumonia. The results showed a high accuracy of 99.4%; this was due to the small dataset size used in their study. Meanwhile, the authors in Kini et al. [38] conducted their study using VGG16 on a dataset containing 12,146 CT scans. In their study, they detected a number of issues from healthy cases and non-healthy cases, with pneumonia being one of them. The results showed high classification accuracy when detecting pneumonia. The authors in Li et al. [39] conducted a study using VGG16 on a dataset containing 7,000 X-ray images. They achieved classification on three classes (i.e., COVID-19, infected by pneumonia, and non-infected by pneumonia). Their results showed an accuracy of 93.57%. The researchers in Luz et al. [40] implemented the classic ImageNet dataset such as ResNet and VGGs. Although its presentation as a small partition may negatively affect other common architectures such as ResNet and VGGs, their results achieved a high accuracy of 93.9%.

The researchers in Shah and Shah [41] conducted a study using DenseNet 121 on dataset contains 112,120 chest X-ray images. Whereas the images were resized into 224 × 224 and normalized using metrics from the ImageNet16 training dataset. Their aim is to detect pneumonia/non-pneumonia images from (14 classes including other lung disorders), whereas the images in the classes were quite unbalanced. The results showed an F1-score of 0.435 and an accuracy of 0.76 when tested 420 images. One of the studies that utilized of using deep-learning models in the field of detecting pneumonia using X-ray images is in Barhoom and Abu-Naser [42]. They used number of CNN architectures like: CNN1, CNN2, DensenNet_121, VGG-16, Resnet_50, and Inception_V3 to extract features. Researchers in Chhabra and Kumar [43] proposed an efficient convolutional neural network based on mutual learning of Resnet-50 network for pneumonia detection using the restorative image method. The dataset is imported from Kaggle-based open-source dataset. They used MobileNet architecture to detect pneumonia/non-pneumonia classes based on dataset contains 5863 chest X-ray images. They applied the necessary changes in the updated manuscript.

To sum up, previous studies have proposed a variety of methods, often focusing on architectural design or transfer learning. In contrast, this study evaluates two pre-trained CNN models, namely ResNet-50 and Inception V3, while also incorporating data augmentation, dropout regularization, and four different image filters. The results of this study are promising and provide a modest improvement over the current state of the art.

3. Methodologies

This section explains the following subsections. Dataset and data augmentation, filters and dropout layer, pneumonia prediction using CNNs models, performance measures, and the proposed method.

3.1. Dataset and Data Augmentation

To achieve reliable performance, a large number of images is typically required to ensure optimal training of pre-trained CNN models. However, since a large size of dataset is not available, the techniques of data augmentation is considered to increase the size of the training dataset artificially (i.e. chest X-ray images) and introduce diversity in data. Data augmentation is implementing a set of changes to the original images, and it is used in this study to train the pneumonia class images that will increase the dataset size, which makes the proposed model more generalizable and robust under diverse conditions. Table 1 shows total size for data after data-augmentation, this is to enhance the ability of the model to classify pneumonia class of non-pneumonia class. Data augmentation was not applied to the test images and validation dataset. Data augmentation types used in this study are illustrated in Figure 1, which include: 1) Randomly rotates the image within a specified range (up to 20 degrees in this case). 2) Width Shift: Shifts the image horizontally by a certain fraction of the total width (up to 20%). 3) Height Shift: Shifts the image vertically by a certain fraction of the total height (up to 20%). 4) Shear: Applies shear transformations, which slant the shape of the image (up to 20%). 5) Zoom: Randomly zooms into images (up to 20%). 6) Horizontal Flip: Randomly flips the images horizontally.

In our experiments, the pre-trained models used included ResNet50 and Inception v3. They were applied on chest X-ray datasets images that contain 5840 images. The dataset was imported from Kermany [3] and the images are grouped as follows: training (PNEUMONIA: 3875, NON-PNEUMONIA: 1341), and Test dataset (PNEUMONIA: 390, NON-PNEUMONIA: 234).

The total experiments conducted in this study is 144 experiments, which are as follows: (CNN models) * 6 (data augmentation) * 4(filters) * 3(Classifiers).

3.2. Filters and Dropout Layer

Four filters are used to reduce image noise and smooth images. Each has its own equation, as illustrated next. Figure 2 shows the influence of filters on the original image. A "hot" color map (hot CMap) is demonstrated in Figure 2, and it typically ranges from black to red, yellow, and white, displaying lower to higher values of the difference from the original images for

each filter type. The hot CMap helps visualize where the changes (due to the blurring filter) have been performed in the image. More investigation is needed on the hot color map to find its influence on detection.

3.2.1. Gaussian Filter

This filter is a linear filter that is used to reduce noise or to create a smoothing effect on an image by averaging pixels within a neighborhood, where the weights are determined by a Gaussian distribution, and it is known as Gaussian Blur [44-46]. In general, it softens the image, reduces fine details, and blurs edges. Equation 1 displays the formula of the Gaussian filter.

$$G(x,y) = \frac{1}{2\delta^2} . exp^{\left(-\frac{x^2+y^2}{2\delta^2}\right)} \quad (1)$$

Where: x and y are the pixel coordinates relative to the center of the filter (usually the center is at (0,0)). While σ is the standard deviation of the distribution for the spread (blur intensity) of the Gaussian filter.

Table 1.
The total Size for training data after Data-Augmentation.

Data Type	Pneumonia	Non-Pneumonia	Total
Original Training Data	3875	1341	5216
Augmented Training Data	23250	8046	31296

3.2.2. Bilateral Filter

It is a non-linear filter that preserves edges while smoothing and reducing noise. It considers both spatial distance (how far apart pixels are) and intensity difference (how similar the pixel values are) when calculating the average [47]. In general, smooths the image while preserving edges. Equation 2 displays the formula of the bilateral filter.

$$I'(x,y) = \frac{1}{w_p} \sum_{i=-k}^{k} \sum_{j=-k}^{k} exp\left(-\frac{(x-i)^2 2+(y-j)^2}{2\delta^2}\right) * \quad exp\left(-\frac{(I(x,y)-I(i,j)^2}{2\delta^2}\right) * \quad I(i,j) \quad (2)$$

Where:

- I′(x,y): it is the value of filtered (output) data in pixel at position (x,y).
- I(x,y): is the input value in pixel at position (x,y).
- I(i,j): is the pixel value at a neighboring pixel (i,j).
- Σs: is the spatial standard deviation, controlling the extent of the spatial window (how far neighbors influence each other).
- σr: is the range standard deviation, controlling how much pixel value differences influence the weighting.
- Wp: It is a normalization factor to ensure that the sum of the weights equals 1, as illustrated in Equation 3.

$$w_{p=} \sum_{i=-k}^{k} \sum_{j=-k}^{k} exp\left(-\frac{(x-i)^2 2+(y-j)^2}{2\delta_d^2}\right) exp\left(-\frac{(I(x,y)-I(i,j)^2}{2\delta_r^2}\right) \quad (3)$$

Where: K defines the size of the filter kernel (usually a square matrix with a side length of 2K+1)

3.2.3. Median Filter Using Skimage

It is a nonlinear filter and works by replacing the pixel value with the median of its neighbors. It is particularly effective at removing salt and pepper noise. It preserves edges better than linear filters (such as Gaussian) because it does not blur the image as much. The window size determines the amount of smoothing applied (larger windows remove more noise but increase blur) [48, 49].

Given an image I, the median filter replaces each pixel at position (x,y) with the median of the pixel values in a window of size 2k+1 centered at (x,y). In general, it removes salt-and-pepper noise. Equation 4 displays the formula for the median using the skimage filter.

$$Iout(x,y)=median(I(x+i,y+j)) \quad for\ i,j \in [-k,k] \quad (4)$$

where:

- I(x,y): it is the pixel value at (x,y).
- Iout(x,y): is the output pixel value at (x,y).
- The neighborhood values: defined by the window of size 2k+1 centered around (x,y).
- Median (·): it computes the median of the pixel values in the window.

3.2.4. Median Filter using OpenCV

This filter is used to remove noise, especially salt and pepper noise. It replaces the pixel value with the median value of the neighboring pixels. It is significantly improved and faster compared to the Skimage implementation, especially for larger images. The main difference is that the OpenCV implementation allows you to specify the kernel size, which affects the size of the local neighborhood for the median calculation [49-51]. In general, reduces noise while maintaining edges. Equation 5 displays the formula of Median using the OpenCV filter.

$$Iout(x,y)=median(\{I(x+i,y+j) \ /i,j \in [-k,k]\}) \quad (5)$$

Where:

- I(x,y): it is the pixel value at position (x,y) of the input image.
- Iout(x,y): is the output pixel value at location (x,y).
- K: half the size of the kernel (e.g., for a 3×3 kernel, k=1).
- Median (.): it computes all the pixel values in the neighborhood window, and is a square of size (2k+1)×(2k+1).

Despite the equations for median using skimage and median using opencv are the same but the differences lie in the implementation as follows [49-51]:

- Skimage: The size and shape of the neighborhood pixels are specified by e.g., square (), disk (). This means it requires a neighborhood parameter (e.g., square (3)) for the function API, and this makes it more flexible in terms of neighborhood shapes
- OpenCV: The kernel size must be an odd single integer (e.g., 3, 5, 7, etc.), and it represents a square kernel. This means that it only requires the kernel size as a parameter, and this makes it less flexible in terms of neighborhood shapes.

3.2.5. Dropout layer

A dropout layer is known as a regularization technique that used in neural networks to prevent overfitting during training. It works by dropping a random portion of neurons into a layer during each training iteration. This lets the network to depend on different subsets of neurons, producing the model more robust and preventing it from over-relying on any one neuron or feature [52]. The next points explain how it works:

- For each iteration during training, the Dropout layer randomly drops neurons out, which means it sets a fraction of the input units to zero.
- The remaining neurons will be scaled up to ensure that the expected output remains the same.
- During testing (or inference), no neurons are dropped out. Instead, the network uses all neurons.

3.3. Models for Pneumonia Prediction Using CNNs

A pre-trained CNN model is designed to be trained on a variety and large dataset of images, and this data is then saved for the purposes of the classification process, which known as a network. The output of CNN model is extracted features for an input image (i.e. chest x-ray images). The main goal of feature extraction is to obtain essential features with distinct valuable information [53, 54]. In this study, the features are extracted using the pre-trained Resnet50 and Inception V3.

Each of CNNs used in this study (i.e., ResNet50 and InceptionV3) has distinct architecture, philosophies, and strengths. The difference between these two models is that the ResNet50 is used for deep networks with complex features. However, InceptionV3 is used for applications that require efficiency and saving in computations without sacrificing much accuracy. In the following paragraphs, a detailed explanation of each of the CNN model structures used in the study is provided [55-57].

ResNet 50 is considered one of the most powerful deep neural networks. ResNet has achieved outstanding performance results in the 2015 ILSVRC Classification Challenge. Additionally, ResNet 50 has shown high efficiency in detection tasks. Both ResNet 50 and Inception v3 architectures have different variations, all using the same fundamental idea, but employing different parameters, numbers of layers, as well as different input sizes [55-57].

Table 2 shows information about CNN models that used in the study. The assumed input size for Reset50 is 224×224×3. Each residual block has three convolutional layers: 1×1, followed by a 3×3, and then 1×1 convolutional layers. The 1×1 convolutional layers are used to reduce the dimensionality before the 3×3 and then recover it afterwards. This design maintains the flow of information while managing the model complexity. The architecture is designed to allow a deeper network of 50 total layers, using skip connections to combat the disappearing gradient problem, and consisting of multiple convolutional layers, and batch normalization, and ReLU, pooling, FC layers. Using convolutional layers (1×1) allows for efficient computation and to improve training performance [55].

InceptionV3 is developed by Google, which uses a composite scaling method. It is goal to optimize the computational efficiency while achieving high performance. The assumed input size for Inception v3 is (299×299×3). Inception has 48 layers that includes convolutional layers, pooling, activation layers, batch normalization, and FC layers. It has approximately 23 million, the larger of the parameters number indicate to the more complex the model; it also means the model requires more memory and computation. All dimensions of the network (depth, width, and resolution) are scaled uniformly to fit a specific resource constraint. The model uses a combination of convolutions with multiple kernel sizes (e.g., 1x1, 3x3, 5x5) in parallel in the same layer, which allows the model to efficiently learn features at different scales without excessively increasing the number of parameters. It utilizes factorized convolutions like 3x3 and 1x1 convolutions, which reduce computational complexity and the number of parameters while still extracting useful features [55-57].

The output layer of each model consists of 1000 neurons, producing a distribution over 1000 classes. Each output neuron will correspond to one of the classes in the dataset [55-57].

Table 2.
The CNN models descriptions used in this study.

CNN	# of Layers	Parameters (millions)	Input	Output
ResNet50	50	~25.6	224×224×3	1000
Inception V3	48	~23	299×299×3	1000

3.4. Research questions and Performance Measures

The analysis of this research will be achieved based on two research questions as follows.

First question (RQ1): To what degree will the extracted features using image filters based on optimized CNN models (ResNet50 and InceptionV3, which are applied in this research), Dropout layer, Dense layer, and data augmentation influence the enhancement of automated detection of pneumonia? This question intends to demonstrate the effect of the proposed method on classifying the input data based on images as infected or non-infected.

Second question (RQ2): To what degree will the proposed method be comparable to the most recent and relevant researches in pneumonia? This question measures the efficiency of the proposed method when compared to searches have been conducted in pneumonia.

A confusion matrix is used for measuring the performance of the proposed model. Based on the predictions, the confusion matrix displays the accurate instances of the model that aim to predict a class label for each instance. The values in confusion matrix range between [0-1]. Next, the explanation for metrics used in the evaluation as follows [58, 59]:

Accuracy is one of the most significant measures for evaluating the model performance. The ratio of total correct instances to total instances is calculated. Equation 6 shows the equation for accuracy.

$$Accuracy=(TP+TN)/(FP+FN+TP+TN) \quad (6)$$

Precision is the percent of TP to the total of TP and FP. It measures the accuracy of the model's positive predictions. Equation 7 illustrates the precision equation.

$$Precision=TP/(TP+FP) \quad (7)$$

Recall is the percent of TP to the total of TP and FN. It measures how well a model can identify all relevant instances from a given dataset. Equation 8 illustrates the recall equation.

$$Recall=TP/(TP+FN) \quad (8)$$

F1score: it is to find the overall performance of the model. It is considered as the harmonic value between recall and precision. Equation 9 illustrates the F1score equation.

$$F1meature=2(Precision*Recall)/(Precision+Recall) \quad (9)$$

Where: (TP) denotes to true positive class, (TN) denotes to true negative class, (FP) denotes to false positive, and (FN) denotes to false negative class.

3.5. Proposed Method

This section describes the proposed models processes in three blocks as shown in algorithm 1 and Figure 3, as follows:

3.5.1. First Block

Step One. Import the Chest x-ray images.

Step Two. Four filters were implemented on the original images. It seems we have five datasets: 1) original images; 2) Gaussian filter images; 3) Bilateral filter images; 4) Median using Skimage filter images; 5) Median using OpenCV filter images.

Step Three. Al the images were entered into set of pre- processing including the images from the original dataset and images after implementing filters, as follows:

i. Resize images to 224x224 pixels. The images are resized to the input size expected by ResNet50/Inception v3.
ii. Data augmentation is applied to the training images, which includes:
   - Rotation: Random rotations of the image by up to 20 degrees.
   - Width Shift: Random shifts of the image in the width direction.
   - Height Shift: Random shifts of the image in the height direction.
   - Shearing: Random shearing transformations.
   - Zooming: Random zooming of the image.
   - Horizontal Flip: Random horizontal flipping.
   - Normalization. A normalization is used in both of the models (Resnet50 and Inception v3), which is applied before feeding the data into the model. This involves scaling pixel values from [0, 255] to the range [-1, 1] and subtracting ImageNet mean values for each RGB channel.

3.5.2. Second Block

Step Four. Fine tuning the model during training for pneumonia and non-pneumonia data. The model is fine-tuned by adding the following layers.

i. Dropout Layer
ii. Dense Layer

Step Five. Feature Extraction: After preprocessing and fine tuning the model, the features were extracted using the models from the images. Each model is used separately.

3.5.3. Third Block

Step Six. Evaluate the model using Classifiers SVM, Random Forest, and Naive Bayes. The metrics used in the evaluation are accuracy, precision, recall, F1 score.

The pooling layer is used for dimensionality reduction. Flatten is used to convert a multi-dimensional output of the final pooling layer (3D tensor of shape: height, width, depth), which is the output of ResNet50/Inception v3, and reshapes it into a 1D vector so that it can be passed into a dense layer. Meanwhile, Dropout is used to prevent overfitting during training.

By randomly dropping a fraction of the neurons during each training iteration, it encourages the model to learn more robust features that are not overly reliant on any specific set of neurons. This enhances the ability of the model to generalize

to new unseen data. While dense layers are used in the model that aggregates features extracted from previous layers to produce a final output that reflects the input's classification. Batch normalization (BN) is included in the architecture of the model to stabilize and accelerate training.

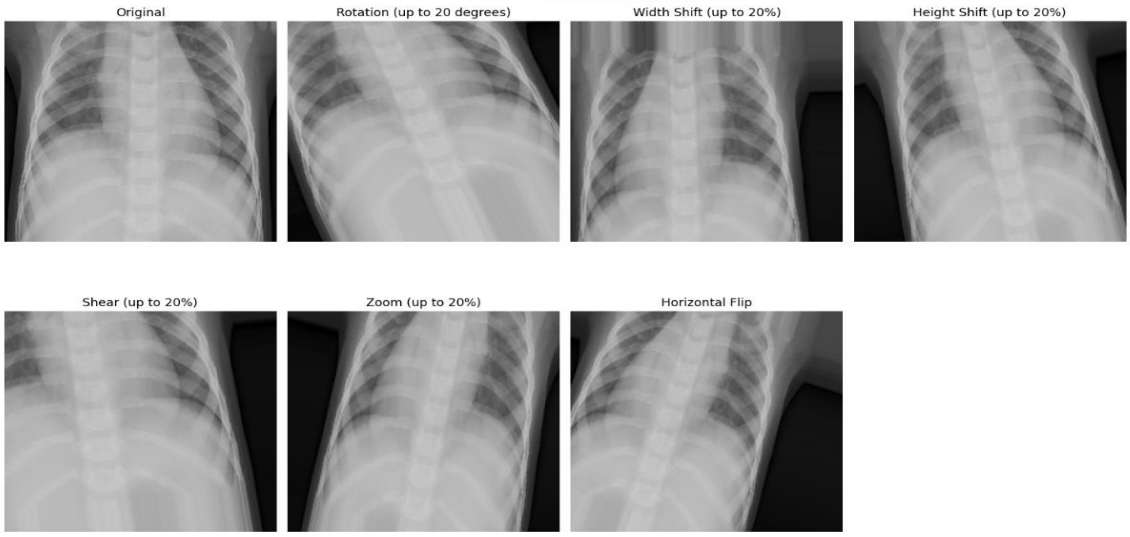

Figure 1.
Data-Augmentation types used in the study.

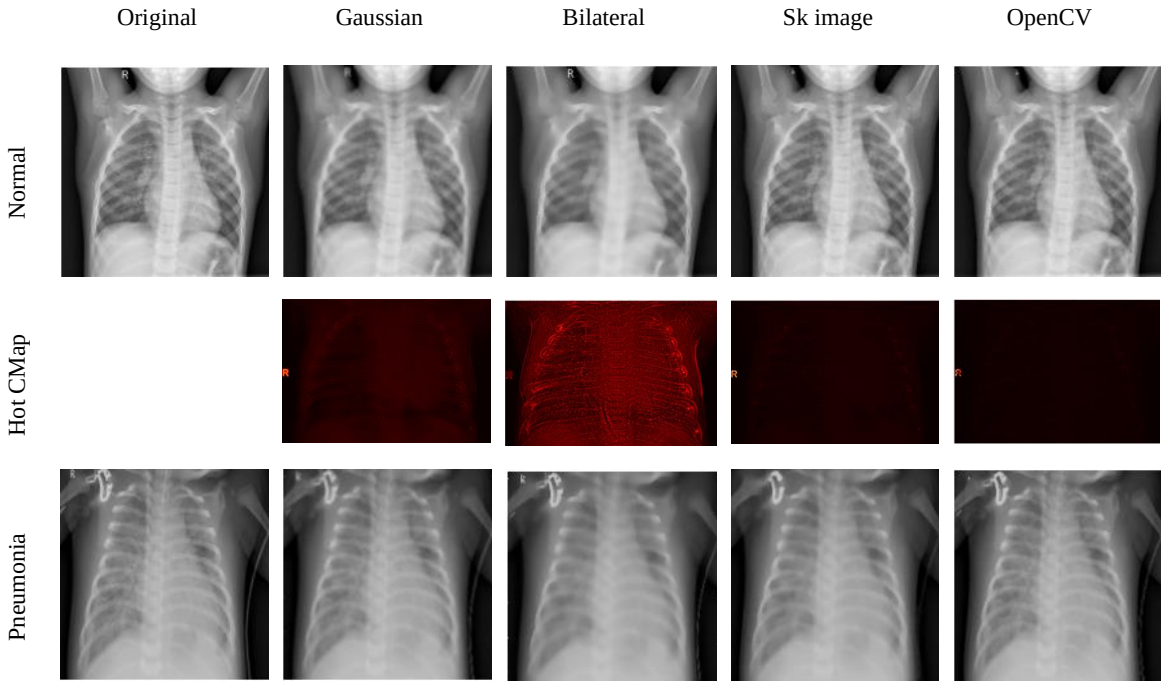

Figure 2.
Filter used in the study.

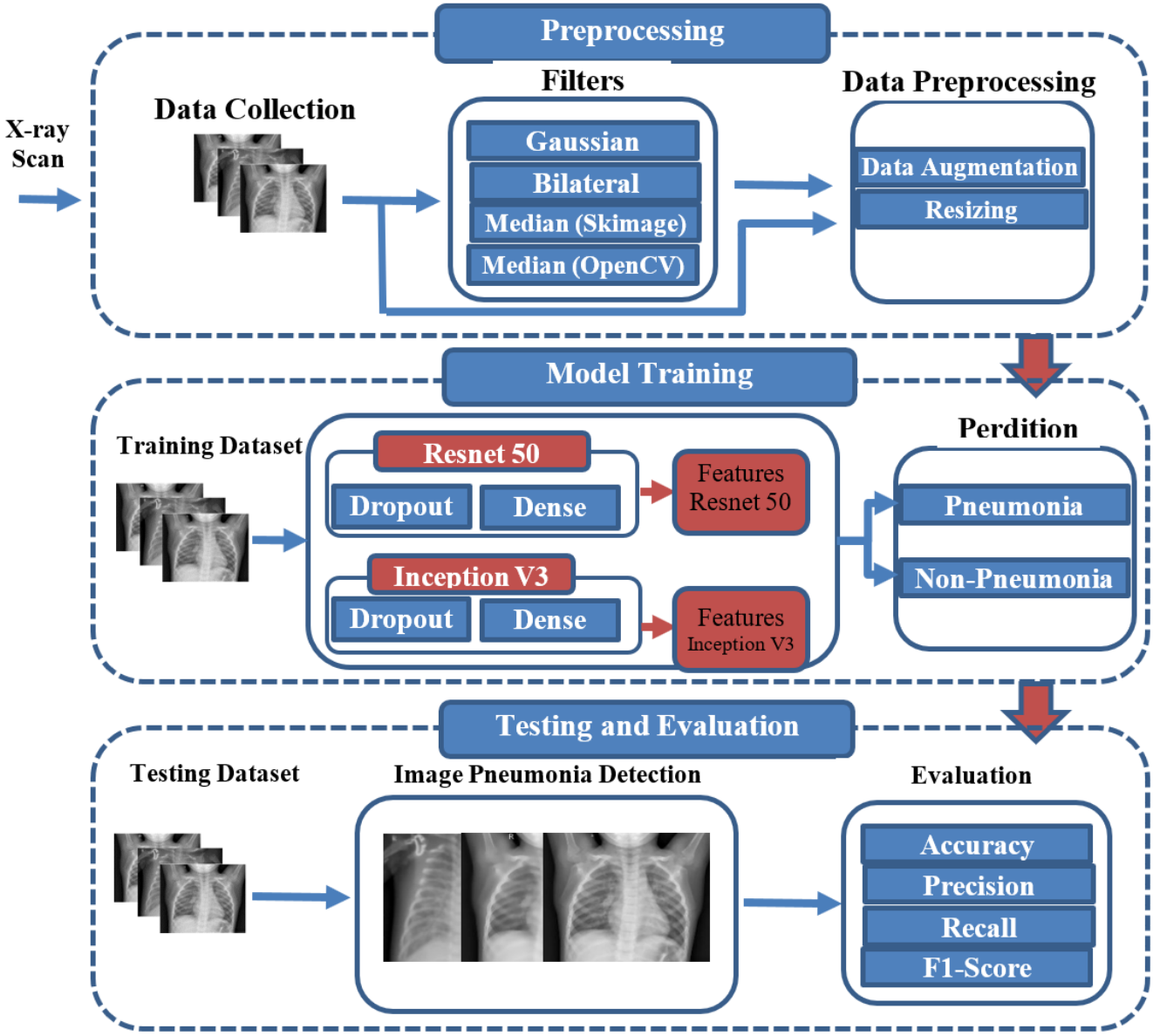

Figure 3.
The proposed Model.

4. Experimental Results and Discussions

This section explains the results of the study represented by answering the two research questions. In the first research question, the results of using four different image filters plus the original datasets (total: five datasets) using the optimized pre-trained models i.e., ResNet 50 and Inception V3 separately. Each has included Drop layer, Dense layer, as well as using different data-augmentation operations will be discussed. While the second question presents the comparison between the results with the most relevant and recent works from the literature. The following metrics will be used for evaluation purposes: Accuracy, Precision, Recall, and F-score. The next sub-sections present the results for each question.

4.1. First Research Question (RQ1)

4.1.1. Results Of Resent 50 Using Dropout

Table 3 displays the results of Recent 50 using Dropout for five datasets: Original dataset, Gaussian filter, Bilateral filter, Median Using Skimage Filter, and Median Using OpenCV Filter. The results showed that the Gaussian filter achieved higher results compared to the results of other datasets. The high results of the Gaussian filter are in favor of SVM compared to other classifiers that scored accuracy (0.975), precision (0.984), recall (0.982), and F1 score (0.983). The second-highest results are from the Bilateral filter in favor of SVM for the accuracy of (0.967). The results for Median Using Skimage Filter were the lowest.

The research in El Asnaoui et al. [60] presented a comparison of results between a set of CNN architectures used for the classification of pneumonia images. In their study, the CNNs included: VGG-16, VGG-19, Densenet_201, Inception_Resnet_V2, Inception_V3, Resnet_50, Mobilenet_V2, and Xception. They conducted their study on 5,856 images (4,273 pneumonia and 1,583 normal). They did not investigate the effects of dropout or data augmentation on the results, nor the effect of using different classifiers; they used softmax only. Therefore, we used the following classifiers in our model:

SVM, RF, and NB. They concluded that the fine-tuned versions of Resnet50, MobileNet-V2, and Inception-Resnet-V2 showed high accuracy for training and validation data (above 96%). However, it was different for CNNs such as Xception, VGG16, VGG19, Inception-V3, and Densenet-201, which showed low accuracy (less than 84%). We align with their results in terms of achieving high accuracy when using Resnet 50; the results were particularly high for the Gaussian filter.

4.1.2. Results of Recent 50 without Dropout

Table 4 displays the results of Recent 50 without Dropout for five datasets: Original dataset, Gaussian filter, Bilateral filter, Median using Skimage Filter, and Median using OpenCV Filter. The results showed that the Gaussian filter achieved high results compared to other datasets. The high results of the Gaussian filter are in favor of SVM compared to other classifiers that scored accuracy (0.975), precision (0.993), recall (0.973), and F1 score (0.983). The second-highest results are from the Bilateral filter in favor of SVM for an accuracy of (0.97). The lowest performance was for the Median using the Skimage Filter.

In general, the results indicate that there is a positive influence when not using the Dropout layer based on ResNet 50. It is still necessary to conduct further investigation on Dropout, as it is recommended to be used to prevent overfitting [61].

Algorithm 1 Features extraction from the models: ResNet50/ Inception V3

Input: Chest x-ray images.

Output: Classification results including accuracy, precision, recall, and F1 score.

1. Process start

2. Import the dataset (Chest x-ray images).

3. Apply the following filters to each image in the dataset based on the original dataset (i.e., Gaussian Filter, Bilateral Filter, Median Filter using skimage, Median Filter using OpenCV).

4. Resize each image to 224x224 pixels.

5. Apply Data augmentation to the training images (i.e., Rotation rotations, Width Shift Randomly in the width direction, Height Shift Randomly in the height direction, Shearing Randomly, Zooming Randomly, Horizontal Flip Randomly, and Normalize the data before send them to the models (Resnet50 and Inception v3.

6. Add a Dropout Layer to the model to reduce overfitting.

7. Add a Dense Layer for classification at the final layer of the network.

8. Use both separately: (ResNet50 and Inception V3) are used to extract features from each image in the datasets: (i.e., Original dataset (no change to the image), Gaussian Filter, Bilateral Filter, Median Filter using the skimage library, and Median Filter using the OpenCV library).

9. Train and evaluate classifiers on the extracted features using the following models: (i.e., Support Vector Machine (SVM), Random Forest, and Naive Bayes

10. Evaluate each classifier based on the following performance metrics: (i.e., Accuracy, Precision, Recall, F1 Score.

11. End Algorithm

There are a number of studies supporting the idea of using filters on the original images to enhance accuracy, such as El Asnaoui et al. [60]. For example, there is a study conducted by Giełczyk et al. [62] to detect pneumonia without using a dropout layer on the following datasets: 1) Original dataset, 2) Gaussian blur + histogram equalization, 3) Bilateral filter + histogram equalization. Despite some differences between our model and their model, such as the number of dense layers: in our model (1), but they used (3 units and 512 units). Also, regarding the classifiers, we used three classifiers, but they used only softmax. Increasing the number of dense layers can increase accuracy. Adding more parameters to deep learning models makes them more prone to overfitting because they have a higher ability to memorize training data rather than learning underlying patterns [61]. Their results found that the accuracy was 0.9515, 0.9877, and 0.9725 for original, Gaussian, and bilateral filter respectively.

Another study was conducted to detect pneumonia in chest x-ray images [63]. In their study, the ratio of their training-test data used is 80% to 20%. Their model is trained for 50 epochs. Increasing the number of epochs leads the model to overfit its training data [64]. Their results showed that the classification using a Gaussian filter scored an accuracy of 92.98%, precision (0.94), recall (0.92), and f1-score (0.93). For the original dataset (non-filter), the model scored an accuracy of 91.94%, precision (0.95), recall (0.92), and f1-score (0.94). In our model, we used different classifiers, a train-test splitting data ratio (70% to 30%), and used 10 epochs for training the model to ensure that the results are not overfitting. In our model, five datasets were used; one for original data, and four for different filters applied to the original. We also used a dropout layer and a model without a dropout layer.

To sum up, therefore, the results of accuracy can be enhanced when using filters and ResNet 50. There is no significant difference between using a dropout layer or not in the case of using ResNet 50. Our results align with the aforementioned studies that indicate high accuracy for the Gaussian filter compared to the non-filter. Based on that, we can conclude that using the right filters may greatly increase classification accuracy [28].

4.1.3. Results of Inception V3 using Dropout

Table 5 displays the results of Inception V3 using Dropout for five datasets: Original dataset, Gaussian filter, Bilateral filter, Median Using Skimage Filter, and Median Using OpenCV Filter. There is no big influence of performance when using filters compared to non-filters (original dataset). The results were slightly similar for the original dataset and the results of other filters. When make a comparison between filters, Gaussian filter has best influence and scored high. The result of Gaussian filter is in favor of SVM compared to other classifiers that scored of accuracy (0. 9661), precision (0. 9745), recall

(0. 9788), and f1 score (0. 9767). The results for non-using filter are in favor of SVM (0.9764 of accuracy).

Table 3.
The Results of Resent 50 using Dropout.

Datasets	Classifiers	Accuracy	Precision	Recall	F1 Score
Original Dataset	SVM	0.9527	0.9757	0.9585	0.9671
	NB	0.9495	0.9808	0.9488	0.9646
	RF	0.9208	0.9316	0.9612	0.9461
Gaussian Filter	SVM	0.9751	0.9841	0.9815	0.9828
	NB	0.9700	0.9910	0.9673	0.9790
	RF	0.9585	0.9717	0.9709	0.9713
Bilateral Filter	SVM	0.9674	0.9807	0.9747	0.9777
	NB	0.9604	0.9892	0.9563	0.9725
	RF	0.9489	0.9651	0.9651	0.9651
Median Using Skimage Filter	SVM	0.8351	0.8254	0.9204	0.8703
	NB	0.8351	0.8154	0.9381	0.8724
	RF	0.7713	0.8302	0.7788	0.8037
Median Using OpenCV Filter	SVM	0.9700	0.9791	0.9799	0.9795
	NB	0.9687	0.9832	0.9738	0.9785
	RF	0.9540	0.9710	0.9659	0.9685

Table 4.
The Results of Resent 50 Without Dropout.

Datasets	Classifiers	Accuracy	Precision	Recall	F1 Score
Original Dataset	SVM	0.9431	0.9888	0.9320	0.9596
	NB	0.9419	0.9887	0.9303	0.9586
	RF	0.9450	0.9712	0.9523	0.9617
Gaussian Filter	SVM	0.9751	0.9928	0.9726	0.9826
	NB	0.9623	0.9963	0.9515	0.9734
	RF	0.9527	0.9592	0.9762	0.9676
Bilateral Filter	SVM	0.9700	0.9782	0.9808	0.9795
	NB	0.9617	0.9839	0.9633	0.9735
	RF	0.9534	0.9645	0.9721	0.9682
Median Using Skimage Filter	SVM	0.8351	0.8417	0.8938	0.8670
	NB	0.8351	0.8534	0.8761	0.8646
	RF	0.8032	0.8167	0.8673	0.8412
Median Using OpenCV Filter	SVM	0.9687	0.9832	0.9738	0.9785
	NB	0.9661	0.9866	0.9668	0.9766
	RF	0.9527	0.9710	0.9642	0.9676

Table 5.
The Results of Inception V3 Using Dropout.

Datasets	Classifiers	Accuracy	Precision	Recall	F1 Score
Original Dataset	SVM	0.9764	0.9832	0.9841	0.9837
	NB	0.9770	0.9893	0.9788	0.9840
	RF	0.9681	0.9729	0.9832	0.9781
Gaussian Filter	SVM	0.9661	0.9745	0.9788	0.9767
	NB	0.9636	0.9864	0.9629	0.9745
	RF	0.9438	0.9540	0.9691	0.9615
Bilateral Filter	SVM	0.9629	0.9823	0.9668	0.9745
	NB	0.9604	0.9927	0.9528	0.9724
	RF	0.9348	0.9515	0.9598	0.9557
Median Using Skimage Filter	SVM	0.9623	0.9788	0.9694	0.9741
	NB	0.9559	0.9838	0.9555	0.9694
	RF	0.9495	0.9635	0.9677	0.9656
Median Using OpenCV Filter	SVM	0.9585	0.9737	0.9694	0.9716
	NB	0.9502	0.9811	0.9502	0.9654
	RF	0.9367	0.9493	0.9651	0.9571

Table 6.
The Results of Inception v3 without Dropout.

Datasets	Classifiers	Accuracy	Precision	Recall	F1 Score
Original Dataset	SVM	0.9770	0.9919	0.9762	0.9840
	NB	0.9744	0.9955	0.9691	0.9821
	RF	0.9642	0.9728	0.9779	0.9754
Gaussian Filter	SVM	0.9674	0.9830	0.9718	0.9774
	NB	0.9591	0.9908	0.9523	0.9712
	RF	0.9495	0.9689	0.9612	0.9650
Bilateral Filter	SVM	0.9597	0.9771	0.9677	0.9724
	NB	0.9578	0.9874	0.9546	0.9707
	RF	0.9444	0.9584	0.9659	0.9622
Median Using Skimage Filter	SVM	0.9649	0.9823	0.9694	0.9758
	NB	0.9617	0.9892	0.9581	0.9734
	RF	0.9444	0.9600	0.9642	0.9621
Median Using OpenCV Filter	SVM	0.9578	0.9695	0.9729	0.9712
	NB	0.9585	0.9813	0.9616	0.9713
	RF	0.9482	0.9667	0.9624	0.9646

Table 7.
A Comparison Between the Proposed Model and Previous Studies.

#	Methodology	Results	Filter
Nandi and Mulimani [67]	combination of ResNet50 and MobileNet	Ensemble model: Accuracy_DB_1=84.35% Accuracy_DB_2=94.43%	No It uses the model filter (kernels)
Jadhav, et al. [68]	LSTM	Precision= 85%	No
Irfan, et al. [69]	ResNet-50, Inception V3, DenseNet121	DenseNet121: Accuracy_DB_1=71% Accuracy_DB_2=76%	No
Wong, et al. [70]	Inception-ResNet-v2	Accuracy= 93%	No
Yu-Xing, et al. [71]	VGG16, VGG19, AlexNet, ResNet18, ResNet50, Inception V3, DenseNet121	ResNet18: Accuracy= 94.64 %	No
Chouhan, et al. [34]	AlexNet, InceptionV3, ResNet18, DenseNet121 and GoogLeNet	Ensemble model using five pre-trained different architectures and majority voting: Accuracy= 96%	No It uses the model filter (kernels
Reshan, et al. [72]	Resnet_50, Resnet_152 V2, Densenet_121, Densenet_201, Xception, VGG16, Efficientnet, Mobilenet.	MobileNet model: Accuracy_DB_1=94.23% Accuracy_DB_2= 93.75%	No
Manickam, et al. [73]	DenseNet-169+SVM, VGG16, RetinaNet + Mask RCNN, VGG16 and Xception,	ResNet50 model: 93.06% accuracy	No
Wu, et al. [31]	Convolutional Neural Network (CNN) recognition model based on Random Forest	97%	adaptive median filter, Convolutional Neural N etwork (CNN) based Dropout layer
Das et al. [36]	U-NET++ architecture	0.9069	median and Gaussian filters Instead of max pooling, the model uses mixed pooling, a combination of max pool and avg pool.
Monani, et al. [28]	CNN- LSTM, Softmax,	Wiener filter (malaria: 96.57% and pneumonia:96.93%)	Median filter, Gaussian filter, Adaptive median filter and Wiener filter

		Gaussian filter (Blood cell)= 97.79%	
[*]	Resnet 50 Inception V3 Dropout/Dense/ data augmentation 4 filters (no previous studies have the 4 filters using SVM, RF, NB classifiers)	98%	4 Filters: 1)Gaussian filter, 2)Bilateral filter, 3)Median using OpenCV, 4)Median using Skimage filters

Note: [*]: Proposed model.

There is an influence of using Inception V3 on the Median Using Skimage Filter that scored more than 96% in both the Dropout layer and the non-Dropout layer. Unlike what happens when using ResNet 50 on the Median Using Skimage Filter, which scored less than 90% and above 84%.

Despite the results in the study El Asnaoui et al. [60] that says there were low influence of performance the Inception V3 on the Gaussian filter (more than 84% accuracy). Whereas they conducted their study without using a Dropout layer, they used a softmax classifier, and without using pre-processing for the data. While the results of our study proved that the results when using Inception V3 on the Gaussian filter are still high (more than 97%) when compared to the filters. More investigations are required to enhance the accuracy of Inception V3 on datasets using filters. As there are many existing techniques used for image segmentation and edge detection; however, none of the existing methods generated a promising segmentation output [65]. Still, it needs more of investigation, especially to evaluate these models on these filters.

4.1.4. Results of Inception V3 without Using Dropout

Table 6 displays the results of Inception V3 without using Dropout for five datasets: Original dataset, Gaussian filter, Bilateral filter, Median Using Skimage Filter, and Median Using OpenCV Filter. There is no big influence on performance when using Inception V3 on the datasets filters. The results were slightly similar for the original dataset and the results of datasets using filters. The results are slightly similar and considered high, scoring above 97%. The results for the original dataset (non-using filter) are in favor of SVM for the accuracy of (0.9770), precision (0.9919), recall (0.9762), and f1 score (0.9840). While the results of the Gaussian filter are in favor of SVM (0.9674), precision (0.9830), recall (0.9718), and f1 score (0.9774). Still, the results for the Gaussian filter are better compared to other filters, and it has proven to be indispensable in different image detection tasks, which offers a smooth and efficient method to enhance and analyze data-based images [46].

The results of accuracy were enhanced when using Inception V3 on the Median Using Skimage Filter in both (using Dropout layer and non-Dropout layer), compared to the results when using Resnet 50 on the Median Using Skimage Filter. This because Inception V3 is sensitive to smaller, cleaner features in the data, and hence, it might perform better with cleaned-up input data after applying a median filter compared to Resnet 50 that is a deeper network, using residual blocks, which means it focuses on learning progressively more complex abstractions [56, 66].

Our results match with a study that conducted by El Asnaoui et al. [60]. In their study, they compared the results of using the following models: VGG-16, VGG-19, Densenet_201, Inception_ResNet_V2, Inception_V3, Resnet_50, Mobilenet_V2 and Xception. Despite we differ from them in that, they did not investigate the effect of dropout, data augmentation on the results, or the effect of using different classifiers; they used softmax only. Therefore, we used in our model the following classifiers: SVM, RF, and NB. The researchers concluded that the fine-tuned versions of Resnet50, MobileNet-V2, and Inception-Resnet-V2 showed high performance with increased training and validation accuracy (over 96%). In contrast to CNN, Xception, VGG16, VGG19, Inception-V3, and Densenet-201 showed low performance (over 84%). We match with their results in that the model Inception V3 scored less on the datasets with filters. In addition, the second-highest results were high specifically for the Gaussian filter compared to other filters.

4.2. Second Research Question (RQ2)

In addition to the research explained in the section on related works and presented in Table 7, a comparison with more recent and relevant work is provided below.

Recent studies using Inception V3 and ResNet50 to classify pneumonia have demonstrated advances in medical imaging through deep learning approaches. A noteworthy study in Fatema et al. [74] developed a framework that integrates Inception V3 with ResNet50, achieving high performance metrics. They reported 85.5% accuracy, 87% precision, 84% recall, and an F1 score of 85.5% in a multi-class setting that included pneumonia classification among other conditions. In Fatema et al. [74], they achieved lower classification accuracy than what we achieved in our research. This may refer to many reasons for the effect of the following. 1) Using the image filters, 2) using optimized Inception V3 and ResNet50, and 3) using data-augmentation techniques in our study.

The same as achieved in the study [75], that conducted on chest X-ray images using transfer learning models based on Inception V3. They achieved 89.7% of accuracy when classifying pneumonia from other pathological conditions. While in other metrics like: precision, recall, and F1-score showed strong predictive validity, they recommended examining more granular metrics in future research.

In contrast, in a direct classification research of pneumonia in Constantinou et al. [76] using Inception V3 and ResNet50.

They found that Inception V3 achieved a validation accuracy of 78% and an F1 score of 0.75. It is worth noting that these results are highly dependent on the size and quality of the dataset, underscoring the importance of robust preprocessing and optimization techniques for model training and validation.

Recent research using different DL and ML models on pneumonia that has provided insights into performance metrics. A study in Arizmendi et al. [77] aimed to distinguish viral, bacterial, and non-viral cases from chest x-ray images analyzed using CNNs. Their results demonstrated an accuracy of 91.02%, precision of 97.73%, recall of 98.03%, and F1 score of 97.88%. they used dimensionality reduction techniques to enhance classification performance and to present an efficient methodology for classifying pneumonia across different etiological factors i.e., smoothing and chi-square.

Another research conducted on pneumonia in Serin et al. [78] applied ML techniques to classify pneumonia in children using clinical data. They achieved an accuracy ranging [77% - 88%] depending on the various clinical features like age and hypoxia. Despite the limitations of detailed performance metrics like precision and recall, this study highlights the importance of structured data analysis in improving the accuracy of pneumonia diagnosis prediction. The comparison with the previous research confirms the reasons that make the results of our research is more reliable as mentioned above in the first paragraph of this section.

Table 7 illustrates a more detailed comparison of the results of this research with the most similar studies conducted in the field of pneumonia detection based on chest X-rays. The details are highlighted in the following points.

- The results obtained from this research are considered high when compared to the results of previous studies in detecting pneumonia using X-ray images.
- The differences in the methodologies used in the studies including this research are huge. The previous studies did not use four different filters, three classifiers (i.e., SVM, RF, NB), Dropout layer, six types of Data-augmentation in their model as conducted in the proposed model.
- The datasets are used in most studies including this research are considered in the same range. But, the data in this research were increased six times by using six types of Data-augmentation technique.
- The total experiments conducted in this study is 144 experiments, which are as follows:2(CNNs models) * 6 (data-augmentation) * 4(filters) * 3(Classifiers).
- It is clear from the table content and the related works, there are shortage in studies conducted on filters that would provide diverse in the methodologies and results.

5. Conclusion

Early detection of pneumonia is essential for reducing diagnostic delays, easing the workload on healthcare professionals, and ultimately saving lives. Traditionally, diagnosis depends on a radiologist's ability to identify signs of pneumonia in chest X-rays, which is both time-consuming and prone to human error, especially when handling large datasets. Therefore, the development of automated diagnostic frameworks in this domain holds significant promise for improving healthcare delivery.

This research aims to improve diagnostic efficiency in regions with limited access to radiologists by facilitating early diagnosis of pneumonia in order to prevent negative consequences (death, etc.). This research is designed based on using two distinct CNN models as part of a deep learning framework for pneumonia detection. These are pre-trained models, ResNet 50 and Inception V3, which take advantage of DL classification of cardiac X-rays into two categories: normal and pneumonia.

To improve performance, the study employed several data preprocessing strategies, including image resizing and data augmentation. Additionally, four commonly used image filters Gaussian, Bilateral, Median (Skimage), and Median (OpenCV) were applied to evaluate their impact on classification accuracy. The influence of Dropout regularization was also investigated to assess its effect on overfitting and generalization.

The results of ResNet 50 using the Dropout layer achieved accuracy values of 98%, 97%, 97%, 95%, and 84% for the Gaussian filter, Bilateral filter, Median using OpenCV, Original dataset, and Median using Skimage filters, respectively. While the results of ResNet 50 for the non-Dropout layer achieved accuracy values of 98%, 97%, 94%, 97%, and 84% for the Gaussian filter, Bilateral filter, Original dataset, Median using OpenCV, and Median using Skimage, respectively.

The results of Inception V3 using the Dropout layer achieved accuracy values of 97%, 96%, 98%, 96%, and 96% for the Gaussian filter, Bilateral filter, original dataset, and Median using OpenCV, and Median using Skimage, respectively. While the results of Inception V3 for the non-Dropout layer achieved accuracy values of 97%, 96%, 98%, 96%, and 96% for the Gaussian filter, Bilateral filter, original dataset, Median using OpenCV, and Median using Skimage, respectively. It is clear that the ResNet model achieves the highest results compared to Inception V3. The results for Median using Skimage with Inception have been enhanced compared to ResNet 50. This may be attributed to Inception V3's ability to capture finer details, and hence, it might perform better with cleaned-up input data after applying a median filter compared to ResNet 50, which is a deeper network using residual blocks, meaning it focuses on learning progressively more complex abstractions [56, 66].

The results of the accuracy can be enhanced when using both the Gaussian filter and the model ResNet 50. There is no significant difference between using a dropout layer or not in the case of using ResNet 50 or Inception V3. Based on that, we can conclude that using the right filters and the model may greatly increase classification accuracy. In addition, the results across all datasets were in favor of using the classifier SVM compared to RF and NB.

In the case of using the model Inception V3, the results in the four filters (Dropout/non-Dropout) were slightly similar. Still, the Gaussian filter is the best compared to other filters, and it has proven to be indispensable in different image detection tasks, offering a smooth and efficient method to enhance and analyze data-based images. Its consistent performance above 97% highlights its robustness. Further investigations are recommended to enhance the accuracy across other filters using different CNN models.

Finally, although various techniques exist for image segmentation and edge detection, many still fall short in delivering consistent and reliable results. Additional research is needed, including further evaluation of visualization techniques such as hot color maps, to assess their potential role in enhancing classification performance.

References

[1] S. Akter and J. F. Shamsuzzaman, "Community acquired pneumonia," *International Journal of Respiratory and Pulmonary Medicine*, vol. 2, p. 2, 2015. https://doi.org/10.23937/2378-3516/1410016

[2] A. McLuckie, *Respiratory disease and its management*. New York: Springer Science & Business Media, 2009.

[3] D. Kermany, *Labeled optical coherence tomography (oct) and chest x-ray images for classification*. United States: IEEE Xplore, IEEE, 2018.

[4] World Health Organization (WHO), *Influenza (Seasonal)*. Geneva, Switzerland: WHO, 2023.

[5] O. Ruuskanen, E. Lahti, L. C. Jennings, and D. R. Murdoch, "Viral pneumonia," *The Lancet*, vol. 377, no. 9773, pp. 1264-1275, 2011. https://doi.org/10.1016/S0140-6736(11)60304-6

[6] World Health Organization (WHO), "Pneumonia in children," Retrieved: https://www.who.int/news-room/fact-sheets/detail/pneumonia. [Accessed 03 January 2025], 2022.

[7] W. Khan, N. Zaki, and L. Ali, "Intelligent pneumonia identification from chest x-rays: A systematic literature review," *IEEE Access*, vol. 9, pp. 51747-51771, 2021. https://doi.org/10.1109/ACCESS.2021.3072277

[8] H. Ezzy, M. Charter, A. Bonfante, and A. Brook, "How the small object detection via machine learning and UAS-based remote-sensing imagery can support the achievement of SDG2: A case study of vole burrows," *Remote Sensing*, vol. 13, no. 16, p. 3191, 2021. https://doi.org/10.3390/rs13163191

[9] Johns Hopkins Coronavirus Resource Center, "Johns Hopkins University & Medicine, Baltimore, MD," Retrieved: https://coronavirus.jhu.edu/. [Accessed 14 September 2022], 2022.

[10] A. Oates *et al.*, "Shortage of paediatric radiologists acting as an expert witness: position statement from the British society of paediatric radiology (BSPR) national working group on imaging in suspected physical abuse (SPA)," *Clinical Radiology*, vol. 74, no. 7, pp. 496-502, 2019. https://doi.org/10.1016/j.crad.2019.04.016

[11] G. Deng and L. Cahill, "An adaptive Gaussian filter for noise reduction and edge detection," in *1993 IEEE Conference Record Nuclear Science Symposium and Medical Imaging Conference*, 1993: IEEE, pp. 1615-1619.

[12] M. Yaseliani, A. Z. Hamadani, A. I. Maghsoodi, and A. Mosavi, "Pneumonia detection proposing a hybrid deep convolutional neural network based on two parallel visual geometry group architectures and machine learning classifiers," *IEEE Access*, vol. 10, pp. 62110-62128, 2022. https://doi.org/10.1109/ACCESS.2022.3197220

[13] W. H. Self, D. M. Courtney, C. D. McNaughton, R. G. Wunderink, and J. A. Kline, "High discordance of chest x-ray and computed tomography for detection of pulmonary opacities in ED patients: implications for diagnosing pneumonia," *American Journal of Emergency Medicine*, vol. 31, no. 2, pp. 401-405, 2013. https://doi.org/10.1016/j.ajem.2012.10.029

[14] A. Ticinesi *et al.*, "Lung ultrasound and chest x-ray for detecting pneumonia in an acute geriatric ward," *Medicine*, vol. 95, no. 27, p. e4153, 2016. https://doi.org/10.1097/MD.0000000000004153

[15] E. Çallı, E. Sogancioglu, B. van Ginneken, K. G. van Leeuwen, and K. Murphy, "Deep learning for chest X-ray analysis: A survey," *Medical Image Analysis*, vol. 72, p. 102125, 2021. https://doi.org/10.1016/j.media.2021.102125

[16] D. Berliner, N. Schneider, T. Welte, and J. Bauersachs, "The differential diagnosis of dyspnea," *Deutsches Ärzteblatt International*, vol. 113, no. 49, p. 834, 2016. https://doi.org/10.3238/arztebl.2016.0834

[17] F. A. Mettler Jr, W. Huda, T. T. Yoshizumi, and M. Mahesh, "Effective doses in radiology and diagnostic nuclear medicine: a catalog," *Radiology*, vol. 248, no. 1, pp. 254-263, 2008. https://doi.org/10.1148/radiol.2481071451

[18] Z. Hu, Z. Yang, K. J. Lafata, F. F. Yin, and C. Wang, "A radiomics-boosted deep-learning model for COVID-19 and non-COVID-19 pneumonia classification using chest x-ray images," *Medical Physics*, vol. 49, no. 5, pp. 3213-3222, 2022. https://doi.org/10.1002/mp.15531

[19] L. Wang *et al.*, "Trends in the application of deep learning networks in medical image analysis: Evolution between 2012 and 2020," *European Journal of Radiology*, vol. 146, p. 110069, 2022. https://doi.org/10.1016/j.ejrad.2021.110069

[20] S. Ben Atitallah, M. Driss, W. Boulila, A. Koubaa, and H. Ben Ghezala, "Fusion of convolutional neural networks based on Dempster–Shafer theory for automatic pneumonia detection from chest X-ray images," *International Journal of Imaging Systems and Technology*, vol. 32, no. 2, pp. 658-672, 2022. https://doi.org/10.1002/ima.22596

[21] M. Iori *et al.*, "Mortality prediction of COVID-19 patients using radiomic and neural network features extracted from a wide chest X-ray sample size: A robust approach for different medical imbalanced scenarios," *Applied Sciences*, vol. 12, no. 8, p. 3903, 2022. https://doi.org/10.3390/app12083903

[22] Z. Salahuddin, H. C. Woodruff, A. Chatterjee, and P. Lambin, "Transparency of deep neural networks for medical image analysis: A review of interpretability methods," *Computers in Biology and Medicine*, vol. 140, p. 105111, 2022. https://doi.org/10.1016/j.compbiomed.2021.105111

[23] P. Malhotra, S. Gupta, D. Koundal, A. Zaguia, M. Kaur, and H.-N. Lee, "Deep learning-based computer-aided pneumothorax detection using chest X-ray images," *Sensors*, vol. 22, no. 6, p. 2278, 2022. https://doi.org/10.3390/s22062278

[24] A. Sedik, M. Hammad, F. E. Abd El-Samie, B. B. Gupta, and A. A. Abd El-Latif, "Efficient deep learning approach for augmented detection of Coronavirus disease," *Neural Computing and Applications*, vol. 34, pp. 1-18, 2022. https://doi.org/10.1007/s00542-022-07081-7

[25] N. Subramanian, O. Elharrouss, S. Al-Maadeed, and M. Chowdhury, "A review of deep learning-based detection methods for COVID-19," *Computers in Biology and Medicine*, vol. 143, p. 105233, 2022. https://doi.org/10.1016/j.compbiomed.2021.105233

[26] X. Lu and Y. Zhang, *An improved canny detection method for detecting human flexibility* (Intelligent IoT Systems in Personalized Health Care). Elsevier. https://doi.org/10.1016/B978-0-12-821187-8.00008-3, 2021.

[27] S. Paris, *A gentle introduction to bilateral filtering and its applications* (ACM SIGGRAPH 2007 courses). ACM. https://doi.org/10.1145/1281500.1281602, 2007.

[28] U. J. Monani, S. Samanta, M. K. Gourisaria, and S. Das, "Efficiency analysis of CNN through different filters for medical image classification," in *2024 Second International Conference on Data Science and Information System (ICDSIS)*, 2024: IEEE, pp. 1-7.

[29] S. A. Alshowarah, "Deep learning and statistical operations based features extraction for lung cancer detection system," *Journal of Theoretical and Applied Information Technology*, vol. 102, no. 3, pp. 1-10, 2024.

[30] P. Rajpurkar *et al.*, "Chexnet: Radiologist-level pneumonia detection on chest x-rays with deep learning," *arXiv preprint arXiv:1711.05225*, 2017. https://doi.org/10.48550/arXiv.1711.05225

[31] H. Wu, P. Xie, H. Zhang, D. Li, and M. Cheng, "Predict pneumonia with chest X-ray images based on convolutional deep neural learning networks," *Journal of Intelligent & Fuzzy Systems*, vol. 39, no. 3, pp. 2893–2907, 2020. https://doi.org/10.3233/JIFS-179697

[32] V. Cheplygina, M. De Bruijne, and J. P. Pluim, "Not-so-supervised: a survey of semi-supervised, multi-instance, and transfer learning in medical image analysis," *Medical Image Analysis*, vol. 54, pp. 280-296, 2019. https://doi.org/10.1016/j.media.2019.02.004

[33] E. Ayan and H. M. Ünver, "Diagnosis of pneumonia from chest X-ray images using deep learning," in *2019 Scientific Meeting on Electrical-Electronics & Biomedical Engineering and Computer Science (EBBT)*, 2019: Ieee, pp. 1-5.

[34] V. Chouhan *et al.*, "A novel transfer learning based approach for pneumonia detection in chest X-ray images," *Applied Sciences*, vol. 10, no. 2, p. 559, 2020. https://doi.org/10.3390/app10020559

[35] T. Rahman *et al.*, "Transfer learning with deep convolutional neural network (CNN) for pneumonia detection using chest X-ray," *Applied Sciences*, vol. 10, no. 9, p. 3233, 2020. https://doi.org/10.3390/app10093233

[36] S. Das, S. Bose, R. Jain, and M. Rout, "Light-UNet++: A simplified U-NET++ architecture for multimodal biomedical image segmentation," in *2023 IEEE International Conference on Contemporary Computing and Communications (InC4)*, 2023, vol. 1: IEEE, pp. 1-5.

[37] S. Ahuja, B. K. Panigrahi, N. Dey, V. Rajinikanth, and T. K. Gandhi, "Deep transfer learning-based automated detection of COVID-19 from lung CT scan slices," *Applied Intelligence*, vol. 51, pp. 571-585, 2021. https://doi.org/10.1007/s10462-020-09899-2

[38] A. S. Kini *et al.*, "Ensemble deep learning and internet of things-based automated COVID-19 diagnosis framework," *Contrast Media & Molecular Imaging*, vol. 2022, no. 1, p. 7377502, 2022. https://doi.org/10.1155/2022/7377502

[39] X. Li, W. Tan, P. Liu, Q. Zhou, and J. Yang, "Classification of COVID-19 chest CT images based on ensemble deep learning," *Journal of Healthcare Engineering*, vol. 2021, no. 1, p. 5528441, 2021. https://doi.org/10.1155/2021/5528441

[40] E. Luz *et al.*, "Towards an effective and efficient deep learning model for COVID-19 patterns detection in X-ray images," *Research on Biomedical Engineering*, pp. 1-14, 2021. https://doi.org/10.1007/s42600-021-00151-6

[41] A. Shah and M. Shah, "Advancement of deep learning in pneumonia/COVID-19 classification and localization: A systematic review with qualitative and quantitative analysis," *Chronic Diseases and Translational Medicine*, vol. 8, no. 03, pp. 154-171, 2022. https://doi.org/10.1002/cdt3.17

[42] A. M. Barhoom and S. S. Abu-Naser, "Diagnosis of pneumonia using deep learning," *International Journal of Academic Engineering Research*, vol. 6, pp. 48–68, 2022.

[43] M. Chhabra and R. Kumar, "An efficient ResNet-50 based intelligent deep learning model to predict pneumonia from medical images," in *2022 International Conference on Sustainable Computing and Data Communication Systems (ICSCDS)*, 2022: IEEE, pp. 1714-1721.

[44] A. H. Hamad, H. O. Muhamad, and S. P. Yaba, "De-noising of medical images by using some filters," *International Journal of Biotechnology Research*, vol. 2, no. 2, p. e0136964, 2014.

[45] J. Maucher, "Gaussian filter and derivatives of Gaussian. HOCHSCHULE DER MEDIEN," Retrieved: https://hannibunny.github.io/orbook/preprocessing/04gaussianDerivatives.html, 2021.

[46] Coursesteach, "Computer vision (Part 25) - Gaussian filter. Medium," Retrieved: https://medium.com/@Coursesteach/computer-vision-part-25-gaussian-filter-c81ea05a4630. [Accessed 2024.

[47] S. Paris, P. Kornprobst, J. Tumblin, and F. Durand, "Bilateral filtering: Theory and applications," *Foundations and Trends® in Computer Graphics and Vision*, vol. 4, no. 1, pp. 1-73, 2009. https://doi.org/10.1561/0600000020

[48] S. Van der Walt *et al.*, "scikit-image: Image processing in Python," *PeerJ*, vol. 2, p. e453, 2014. https://doi.org/10.7717/peerj.453

[49] M. Elad, B. Kawar, and G. Vaksman, "Image denoising: The deep learning revolution and beyond—a survey paper," *SIAM Journal on Imaging Sciences*, vol. 16, no. 3, pp. 1594-1654, 2023. https://doi.org/10.1137/S1931156319212218

[50] K. Akhade, "A survey on image denoising techniques," *International Journal of Innovative Science and Research Technology*, vol. 9, no. 2, pp. 689–694, 2024.

[51] S. Manonmani, V. Lalitha, and S. Rangaswamy, "Survey on image denoising techniques," *International Journal of Scientific Engineering and Technology Research*, vol. 5, no. 9, pp. 2278-7798, 2016.

[52] H. Yadav, "Dropout in neural networks," Retrieved: https://towardsdatascience.com/dropout-in-neuralnetworks-47a162d621d9. [Accessed 10. 10. 2023], 2022.

[53] J. Lee, G. Jeon, and Y. Jang, "Feature extraction using deep convolutional neural networks for classification tasks," *Neural Networks*, vol. 158, pp. 58–69, 2023. https://doi.org/10.1016/j.neunet.2023.03.007

[54] J. D. Bodapati and N. Veeranjaneyulu, "Feature extraction and classification using deep convolutional neural networks," *Journal of Cyber Security and Mobility*, vol. 8, no. 2, pp. 261–276, 2019. https://doi.org/10.13052/jcsm2245-1439.825

[55] H. Aziz, "ResNet-50 implementation. Medium," Retrieved: https://pub.aimind.so/resnet-50-implementation-8bde36f2301a. [Accessed 2023.

[56] C. Szegedy, V. Vanhoucke, S. Ioffe, J. Shlens, and Z. Wojna, "Rethinking the inception architecture for computer vision," presented at the Proceedings of the IEEE Conference on Computer Vision and Pattern Recognition, 2016.

[57] A. Brital, "Inception V2 CNN Architecture explained, Medium," Retrieved: https://medium.com/@AnasBrital98/inception-v3-cnn-architecture-explained-691cfb7bba08. [Accessed 2021.

[58] R. Toshniwal, "How to select performance metrics for classification models," Retrieved: https://medium.com/analytics-vidhya/how-to-select-performance-metrics-for-classification-models-c847fe6b1ea3, 2022.

[59] S. A. Hicks *et al.*, "On evaluation metrics for medical applications of artificial intelligence," *Scientific Reports*, vol. 12, no. 1, p. 5979, 2022. https://doi.org/10.1038/s41598-022-09954-8

[60] K. El Asnaoui, Y. Chawki, and A. Idri, *Automated methods for detection and classification pneumonia based on x-ray images using deep learning* (Artificial intelligence and blockchain for future cybersecurity applications). Cham: Springer, 2021.

[61] A. Mueed, "Why are deep learning models with more parameters more prone to overfitting? Quora.com," Retrieved: https://www.quora.com/Why-are-deep-learning-models-with-more-parameters-more-prone-to-overfitting. [Accessed 23 April 2024], 2024.

[62] A. Giełczyk, A. Marciniak, M. Tarczewska, and Z. Lutowski, "Pre-processing methods in chest X-ray image classification," *Plos one*, vol. 17, no. 4, p. e0265949, 2022. https://doi.org/10.1371/journal.pone.0265949

[63] S. Das, S. Samanta, and M. Rout, "Analysis of Pneumonia detection in X-ray images using different filters based Convolution Neural Networks," in *2023 OITS International Conference on Information Technology (OCIT)*, 2023: IEEE, pp. 787-792.

[64] K. Marshall, "How does epoch affect accuracy? Deepchecks Ltd," Retrieved: https://www.deepchecks.com/question/how-does-epoch-affect-accuracy/#:~:text=A%20very%20big%20epoch%20size,begins%20to%20overfit%20the%20data, 2024.

[65] P. Meenakshi, K. Bhavana, and A. K. Nair, "Pneumonia detection using X-ray image analysis with image processing techniques," in *2022 7th International Conference on Communication and Electronics Systems (ICCES)*, 2022: IEEE, pp. 1657-1662.

[66] G. U. Kiran, "Image processing techniques in computer vision. In Futuristic Trends in Computing Technologies and Data Sciences," Retrieved: https://www.researchgate.net/publication/381445195_IMAGE_PROCESSING_TECHNIQUES_IN_COMPUTER_VISION, 2024.

[67] R. Nandi and M. Mulimani, "Detection of COVID-19 from X-rays using hybrid deep learning models," *Research on Biomedical Engineering*, vol. 37, pp. 687-695, 2021. https://doi.org/10.1007/s42600-021-00181-0

[68] A. Jadhav, K. C. Wong, J. T. Wu, M. Moradi, and T. Syeda-Mahmood, "Combining deep learning and knowledge-driven reasoning for chest X-ray findings detection," in *AMIA Annual Symposium Proceedings*, 2021, vol. 2020, p. 593.

[69] A. Irfan, A. L. Adivishnu, A. Sze-To, T. Dehkharghanian, S. Rahnamayan, and H. R. Tizhoosh, "Classifying pneumonia among chest X-rays using transfer learning," in *2020 42nd Annual International Conference of the IEEE Engineering in Medicine & Biology Society (EMBC)*, 2020: IEEE, pp. 2186-2189.

[70] K. C. Wong, M. Moradi, J. Wu, and T. Syeda-Mahmood, "Identifying disease-free chest x-ray images with deep transfer learning," in *Medical Imaging 2019: Computer-Aided Diagnosis*, 2019, vol. 10950: SPIE, pp. 179-184.

[71] T. Yu-Xing *et al.*, "Automated abnormality classification of chest radiographs using deep convolutional neural networks," *NPJ Digital Medicine*, vol. 3, no. 1, pp. 1-9, 2020. https://doi.org/10.1038/s41746-020-0273-z

[72] M. S. A. Reshan *et al.*, "Detection of pneumonia from chest X-ray images utilizing mobilenet model," *Healthcare*, vol. 11, no. 11, p. 1561, 2023. https://doi.org/10.3390/healthcare11111561

[73] A. Manickam, J. Jiang, Y. Zhou, A. Sagar, R. Soundrapandiyan, and R. D. J. Samuel, "Automated pneumonia detection on chest X-ray images: A deep learning approach with different optimizers and transfer learning architectures," *Measurement*, vol. 184, p. 109953, 2021. https://doi.org/10.1016/j.measurement.2021.109953

[74] K. Fatema, S. Montaha, M. A. H. Rony, S. Azam, M. Z. Hasan, and M. Jonkman, "A robust framework combining image processing and deep learning hybrid model to classify cardiovascular diseases using a limited number of paper-based complex ECG images," *Biomedicines*, vol. 10, no. 11, p. 2835, 2022. https://doi.org/10.3390/biomedicines10112835

[75] R. D. Dondapati, T. Sivaprakasam, and K. V. Kumar, "Dermatological decision support systems using cnn for binary classification," *Engineering, Technology & Applied Science Research*, vol. 14, no. 3, pp. 14240-14247, 2024. https://doi.org/10.48084/etasr.7173

[76] M. Constantinou, T. Exarchos, A. G. Vrahatis, and P. Vlamos, "COVID-19 classification on chest X-ray images using deep learning methods," *International Journal of Environmental Research and Public Health*, vol. 20, no. 3, p. 2035, 2023. https://doi.org/10.3390/ijerph20032035

[77] C. Arizmendi, J. Pinto, A. Arboleda, and H. González, "Diagnosis of patients with viral, bacterial, and non-pneumonia based on chest x-ray images using convolutional neural networks," *arXiv preprint arXiv:2503.02906*, 2025. https://doi.org/10.3991/ijoe.v20i16.52895

[78] O. Serin *et al.*, "Advancing primary care for childhood pneumonia: A machine learning-based approach to prognosis and case management," *MedRxiv*, p. 2024.02. 22.24303209, 2024. https://doi.org/10.1101/2024.02.22.24303209